metals

MDPI

Article

Preparation and Analysis of Complex Barrier Layer of Heterocyclic and Long-Chain Organosilane on Copper Alloy Surface

Qian Zhao [1], Tiantian Tang [1], Peilin Dang [1], Zhiyi Zhang [2] and Fang Wang [1,*]

[1] College of Science, Northwest A&F University, Xinong Road No.22, Yangling 712100, China; qianzhao-0918@163.com (Q.Z.); tangtiantian1020@foxmail.com (T.T.); dangpeilin1117@nwsuaf.edu.cn (P.D.)

[2] College of Information Engineering, Northwest A&F University, Xinong Road No.22, Yangling 712100, China; zhangzhiyi@nwsuaf.edu.cn

* Correspondence: wangfang4070@nwsuaf.edu.cn; Tel.: +86-29-8709-2226

Academic Editor: Hugo F. Lopez

Received: 7 June 2016; Accepted: 7 July 2016; Published: 13 July 2016

Abstract: A single electrodeposited film of 6-(3-triethoxysilylpropyl)amino-1,3,5-triazine-2,4-dithiol monosodium (TES) on a copper alloy surface was prepared by the galvanostatic method, then octyl-triethoxysilane (OTES) or hexadecyl-trimethoxysilane (HDTMS) was used to modify the electrodeposited film by the self-assembled technique to fabricate the complex film. The electrodeposition process was inferred by cyclic voltammetry. The single and complex films were characterized by means of contact angle, cyclic voltammetry, Fourier transform infrared spectroscopy (FT-IR), potentiodynamic polarization, electrochemical impedance spectroscopy (EIS) and scanning electron microscope (SEM). The results showed that the contact angle of the complex film covering the copper alloy surface was up to 118.1° compared with 89.4° of the bare copper alloy. The cyclic voltammogram, polarization curves and EIS indicated that the anti-corrosion performance of complex film was better than that of single electrodeposited TES film, and the protection efficiency was up to 90.2%.

Keywords: complex film; cyclic voltammetry; potentiodynamic polarization; anti-corrosion

1. Introduction

Copper and its alloys are extensively used in industry areas because of their high electrical and thermal conductivities, mechanical workability and inactive properties [1]. However, copper and its alloys are inclined to be corroded in various environments [2,3]. Therefore, corrosion decelerating of copper and its alloys is of great importance. In order to achieve this aim, the application of inhibitors is one of the effective approaches to solving the corrosion problems of copper and its alloys. Currently, the most extensive study is choosing proper organic compounds as corrosion inhibitors, such as azoles [4], amines [5] and amino acids [6]. However, most of these corrosion inhibitors are toxic or have an unpleasant smell. Therefore, more and more studies have been carried out to develop environmentally friendly inhibitors [7–9] in recent years. On the other hand, various types of self-assembled singles (SAMs) and self-assembled multi-layers have been developed to be applied in the area of metal protection [10,11]. Among them, silanization based on the use of alkoxysilanes is a typical example in metal pretreatment industries. The formation of silane films is based on the sol-gel process, i.e., the hydrolysis of silanes producing silanols, and the condensation reaction among the silanols or between the silanols and the hydroxylated substrates, forming the Si-O-Si bone structure and Si-O-substrate interfacial layer, respectively. However, some drawbacks of the SAMs are their relatively low thermal and mechanical stability and their propensity for containing molecule-sized defects. Since redox

species can permeate through self-assembled singles on the surface, sufficient protective ability has not been obtainable.

Some organic compounds, which contain functional electronegative groups and π-electrons in triple or conjugated double bonds, play an important role in the corrosion inhibition process [12]. These hetero-atoms, such as sulfur, phosphorus, nitrogen, and oxygen, together with heterocyclic or conjugated aromatics, are known to be an excellent complex with metals or chelate with metals of the transition series. Furthermore, the most synthesized compounds are the nitrogen heterocyclic compounds. Mori studied the corrosion protection properties of triazinedithiols on the various metal substrates by adsorption and electrochemical polymerization [13–15]. The experiments showed that polymeric nanofilms prepared by different triazinedithiols had a basic anticorrosion property. Baba investigated the corrosion inhibition of copper by potentiostatic anodization in triazinedithiol solutions [16]. Wang prepared electropolymerized film on a copper alloy surface using 6-*N*,*N*-dibutylamino-1,3,5-triazine-2,4-dithiol monosodium, which showed that the film was more hydrophobic, compact and had excellent protection efficiency [17]. Kang's research indicated that the polymeric film of triazinedithiols on a rough pure copper surface exhibited an excellent super-hydrophobic property [18].

In this study, self-designed and synthesized triazinedithiolsilane is used to prepare the novel heterocyclic silane electrodeposited film of 6-(3-triethoxysilyl-propyl)amino-1,3,5-triazine-2,4-dithiol monosodium (TES) on a copper alloy surface. The novel electrodeposited film was further modified by octyl-triethoxy silane (OTES) or hexadecyl-trimethoxy silane (HDTMS) self-assembled films to obtain the complex films of heterocyclic and long-chain organosilane. Few related studies have been reported so far. The characteristics of single and complex films on copper alloy are analyzed by means of Fourier transform infrared spectroscopy (FT-IR), contact angle, scanning electron microscope (SEM), cyclic voltammetry, potentiodynamic polarization and electrochemical impedance spectroscopy (EIS).

2. Experimental Section

2.1. Materials and Reagents

Test specimens (50 mm × 30 mm × 0.2 mm) of copper alloy (Cu: 88.0%–91.0%; Zn: 9.0%–12.0%) were prepared by cutting a large plate into pieces. All test plates were polished with a series of polishing agents, followed by ultrasonic degreasing in acetone for 15 min and dried in nitrogen stream. The 6-(3-triethoxysilylpropyl)amino-1,3,5-triazine-2,4-dithiol monosodium (TES) was synthesized by the reaction between 6-(3-triethoxysilylpropyl)amino-1,3,5-triazine-2,4-dichloride and NaSH according to the method in the previous study [19]. The molecular structure was shown in Figure 1. Octyl-triethoxy silane (OTES) and hexadecyl-trimethoxy silane (HDTMS) were purchased from Aladdin Reagents (Shanghai, China). All of the chemicals were employed as analytical reagent (AR) without any further purification. Distilled water and ethanol were used as solvents, and sodium carbonate (Na_2CO_3) was used as the supporting electrolyte for electrodeposition. The concentrations of TES and Na_2CO_3 were kept constant at 3 mmol/L and 0.15 mol/L, respectively. The OTES and HDTMS solutions were obtained by dissolving silane (1% vol./vol.) in ethanol (90% vol./vol.) and distilled water (9% vol./vol.). The pH of OTES/HDTMS solution was adjusted to 4.5 by adding acetic acid, followed by being stirred for 1 h, and aged at 35 °C for 24 h to allow the sufficient hydrolysis of OTES/HDTMS.

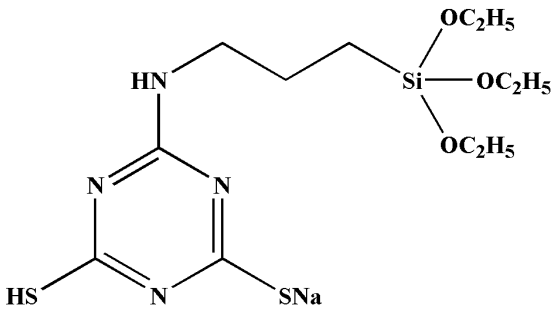


Figure 1. Structure of TES.

2.2. Preparation of Complex Film on Copper Alloy Surface

The electrodeposition of TES monomer was performed using an electrochemical potentiostat (CHI 660C). The electrolytic cell was equipped with a working electrode (copper plate, WE), two counter electrodes (stainless steel plates, CE) and a reference electrode (saturated calomel electrode, SCE). Cyclic voltammetry (CV) for electrodeposited mechanism study was conducted from −0.1 V to 1.1 V at the rate of 20 mV/s in 0.15 mol/L Na_2CO_3 aqueous solution. Galvanostatic electrodeposition was conducted at a current density of 0.02 mA/cm^2 in 0.15 mol/L Na_2CO_3 aqueous solution with TES (3 mmol/L) for 16 min. In this work, all of the potentials were versus to SCE. After the electrodeposition, the working electrode was removed from the electrolytic cell and immediately rinsed by distilled water and ethanol, then dried in air.

Complex film on copper alloy surface was then prepared by the steps as following. The copper alloy covered by TES electrodeposited film was immersed in the hydrolyzed OTES or HDTMS ethanol-water solution for 30 min, followed by being rinsed with ethanol, blow-dried in nitrogen stream and cured for 15 min at 120 °C.

2.3. Characterization

The wettability of copper surface modified by single and complex films was measured by optical contact angle instrument (SL100, Suolun Information Technology Co., Shanghai, China) at room temperature. FT-IR was carried out by attenuated total reflection spectroscopy (TENSOR 37, Bruker, Karlsruhe, Germany). Corrosion tests were investigated by potentiodynamic polarization in 0.5 mol/L NaCl aqueous solution. The exposed area was controlled at 1.0 cm^2. The insulating property of films was studied by cyclic voltammetry from −1.0 V to 0.4 V at the rate of 20 mV/s in 0.1 mol/L NaOH solution. Potentiodynamic polarization was conducted from −1.1 V to −0.7 V with the scanning rate of 5 mV/s. EIS was recorded after 1 h immersion time in 0.5 M NaCl solution under open-circuit potential. The frequency of the potential perturbation was varied from 10^{-2} Hz to 10^3 Hz with the excitation voltage of 5 mV. The surfaces morphologies of blank and copper alloy modified by single and complex films were observed by SEM (JSM-6360LV, JEOL, Tokyo, Japan) at the accelerating voltage of 20 kV, respectively.

3. Results and Discussion

3.1. Electrodeposition of TES Monomer

The electrodeposition process occurring on the copper electrode surface was studied by cyclic voltammetry in 0.15 mol/L Na_2CO_3 aqueous solution (with/without TES monomer) (Figure 2). It was found that the anodic current density of the copper alloy in Na_2CO_3 solution with the TES monomer was lower than that in the blank solution, especially at 1.1 V, and it decreased from 49 mA/cm^2 to 4.9 mA/cm^2. In the cyclic voltammogram of blank solution, only one anodic peak was observed near 0.13 V which indicated the oxidative reaction of the copper surface and the formation of the Cu^+ or Cu^{2+} ions. The larger current density at 1.1 V indicated the electrolysis of water or the dissolution

of copper. However, three anodic peaks were observed in that of the solution with TES monomer. Compared with the blank solution, peak a shifted toward a higher potential. A light yellow film was observed on the copper alloy surface; it was inferred to be the oxidation of the TES monomer and the formation of the Cu-TES complex on the copper alloy surface, depressing the oxidation of the copper. Peak b revealed the electrochemical polymerization of TES monomers [16]. Peak c, observed at 1.1 V, was due to the bubbles produced by the electrolysis of water. The current density of peak c is much lower than that in the blank solution as the thin TES electrodeposited film covered the copper surface, which blocks the charge transfer process. Although about 10% Zn is contained in the copper alloy, the oxidative reaction of Zn occurs at 1.25–1.4 V in the neutral or alkaline solutions to form the passive film [20,21], which will inhibit the reaction between the Zn substrate and compounds in the solution. In the scanning range of the cyclic voltammogram, only copper oxidization can be involved.

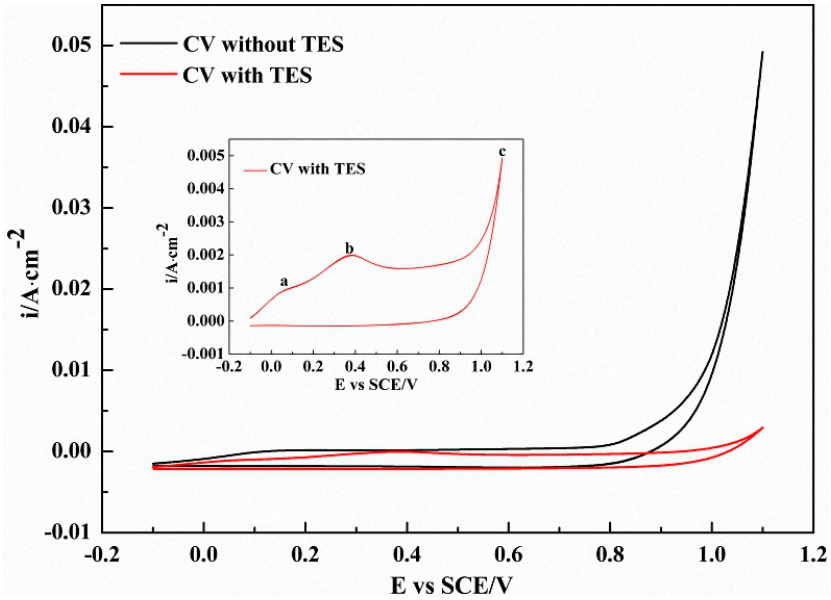


Figure 2. Cyclic voltammogram of copper alloy in 0.15 mol/L Na_2CO_3 aqueous solution with/without TES.

3.2. FT-IR Spectra Analysis

Figure 3 shows the IR spectrum of the copper alloy surface modified by TES and complex film. It can be seen that the bands at 1559 cm^{-1}, 1518 cm^{-1} and 1456 cm^{-1} are assigned to the stretching vibration of –C=N of the triazine rings. It is suggested that TES film is formed on the copper alloy surface. However, the absorption peaks of TES/OTES and TES/HDTMS complex films were significantly weaker than that of the TES self-assembled film, because the silicon hydroxyl of OTES or HDTMS could react with the silicon hydroxyl of TES on the copper alloy surface by condensation, to form excellent complex films, which partly covered the TES self-assembled film. The free hydroxyl stretching vibration peak was distributed in the range of 3500 cm^{-1} to 3700 cm^{-1}. It is noted that single TES film on the copper alloy surface still contained many free hydroxyls. However, the peak intensity in the range of 3500 cm^{-1} to 3700 cm^{-1} decreased obviously after assembling OTES or HDTMS on TES self-assembled film, which means that free hydroxyls in the complex film are greatly decreased, demonstrating the condensation reaction taking place between the unreacted hydroxyl of TES and the hydroxyl of OTES or HDTMS hydrolysis.

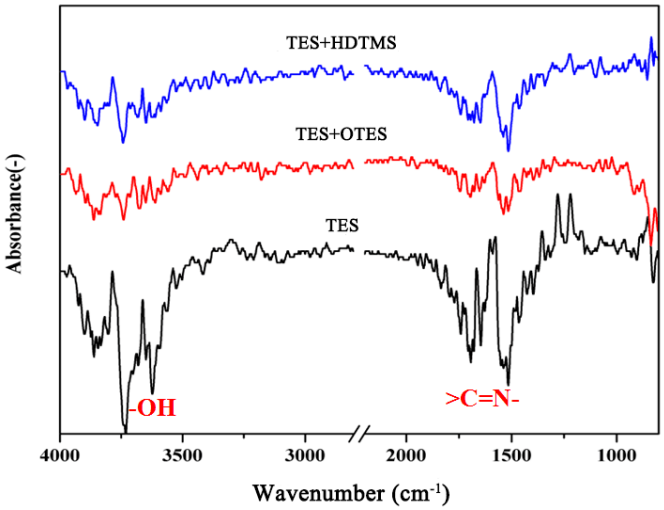


Figure 3. FT-IR spectra of copper alloy surface modified by single and complex films.

3.3. Contact Angle

Figure 4 shows the contact angles of blank, single and complex films covering the copper alloy surface. Compared with the 89.4° angle of the blank, the contact angle of the TES film covering the copper alloy surface is 66.5°, which is attributed to the existence of unbonded hydroxyls on the TES film–covered surface. The contact angles are up to 108.2° and 118.1° for the TES/OTES and TES/HDTMS complex film–modified surfaces, respectively. The result could be attributed to the hydroxyl-provided reaction sites for the further self-assembling of the long-chain organic silane complex film, which led to the formation the Si-O-Si network structure. At the same time, the long-chain part also enhanced the hydrophobicity of the copper alloy surface. The alkyl chain length of HDTMS is longer than that of OTES, resulting in the hydrophobicity of the TES/HDTMS complex film being superior to that of the TES/OTES complex film. According to previous research reports, the hydrophobic property is believed to be due to the presence of the geometric structure at the micro-/nano-meter scale and the functional groups in the top layers which reduce the surface free energy. In this study, the copper alloy surfaces are covered by TES/OTES or TES/HDTMS complex film. The longer $–CH_2CH_3$ terminal group in the top layer makes the surface free energy lower. On the other hand, it is supposed that the micro- or nano-meter structures exist on the surface covered by TES/OTES or TES/HDTMS complex films, which bestow the surface hydrophobicity and can prevent the penetration of water droplets into the substrate. The above results indicated that the hydrophobic cross-linked complex film was formed on the copper alloy surface and it was proposed that the anti-corrosion property of the copper alloy surface modified by the complex film had been enhanced [22].

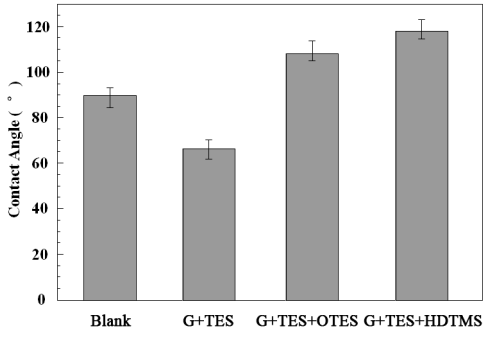


Figure 4. Contact angle of the copper alloy modified by single and complex films.

3.4. Surface Morphology

To further investigate the performance of the complex film, the surface morphologies of the copper alloy surface were observed by SEM, as shown in Figure 5. For the untreated copper alloy surface (Figure 5a), the scratches introduced in the rolling and polishing process were observed. As for the TES electrodeposition film-covered surface (Figure 5b), the scratches on the copper alloy surface were shaded by the TES film to some extent. However, some comparatively large pores and scratches could still be observed. It is deduced that the pores are mainly caused by the imperfect coverage of TES electrodeposited film for the relatively larger steric hindrance of TES molecules and the hydrogen bubbling during the anodic dissolution of copper. Moreover, the hydrolysis process may destroy the film to some extent. Figure 5c,d show the images of TES/OTES and TES/HDTMS complex film-modified surfaces. The surface scratches, pores and large fine intermetallic particles could hardly be seen. In particular, the surface covered by the TES/HDTMS complex film was more homogenous, and the pores were almost covered completely, which was due to the increased thickness of the TES/HDTMS complex film. It is thought that the hydroxyl groups existing in the hydrolyzed OTES or HDTMS react with the silanol groups of the TES electrodeposited film on the copper surface to form the complex films. Therefore, it is concluded that the composite technique of electrodeposition and self-assembling treatment could modify the copper alloy surface effectively.

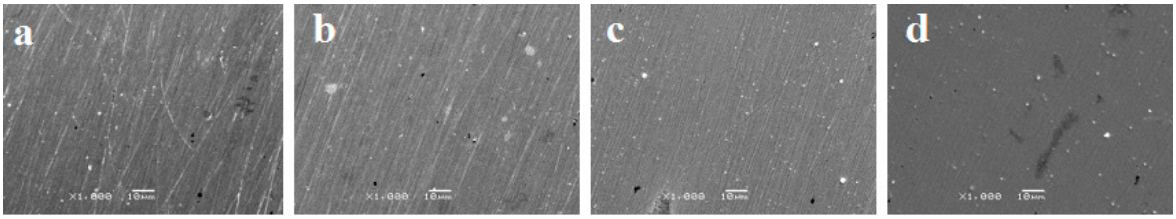


Figure 5. SEM images of copper alloy surface modified by single and complex films. (**a**) Blank; (**b**) TES electrodeposited film; (**c**) TES/OTES complex film; (**d**) TES/HDTMS complex film.

3.5. Cyclic Voltammetry Measurement for the Bare and Modified Copper Surface

The cyclic voltammetry (CV) curves of the copper alloy electrodes unmodified and modified by single and complex films in 0.1 mol/L NaOH aqueous solution are shown in Figure 6. Noticeably, the surface covered with or without film has no significant influence on the general shape of the cyclic voltammograms. For the bare copper alloy, the two obvious activated anodic peaks, I (−0.39 V) and II (−0.18 V and −0.13 V), could be attributed to the continuous formation of Cu_2O and CuO as a result of the electro-oxidation of the basal copper alloy. Cathodic peaks I′ (−0.87 V) and II′ (−0.54 V) resulted from the reduction of Cu_2O and CuO, respectively. Compared with the blank surface, the TES electrodeposited film-covered electrode has relatively lower current peaks, but higher current peaks than complex film-modified electrodes. It is suggested that TES electrodeposited film could have a lower density and more exposed substrate areas. On the other hand, the oxidative reaction currents are largely reduced for the single- and complex film-covered surfaces and their corresponding peak potentials shift in a more positive direction, demonstrating that the behavior of the oxidative reaction of the copper alloy surface modified by single and complex films was highly blocked in alkaline aqueous solution according to the following sequence: TES/HDTMS > TES/OTES > TES > Blank. Among all CV curves of the modified electrodes, the current and area of the TES/HDTMS complex film-covered electrode was the smallest, suggesting the largest resistance against the copper alloy oxidative-reductive reaction compared with the other modified electrodes. It is expected that the TES/HDTMS complex film plays an important role in the protection of the copper alloy substrate from corrosion and oxidation.

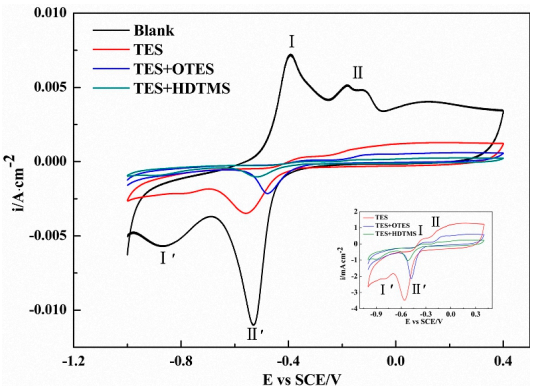


Figure 6. Cyclic voltammograms of copper alloy modified by single and complex films in 0.1 mol/L NaOH aqueous solution.

The previous information can be supported by the change of the anodic peak potentials, the oxidative reaction current density and the area of the cyclic voltammograms. The anodic potentials, current density and area of the cyclic voltammograms of the peaks for blank copper and copper covered by TES single film and TES/OTES or TES/HDTMS complex film are shown in Table 1. After the oxidative reaction of Cu to Cu_2O, the further process of oxidizing Cu_2O to CuO would become much more difficult because of Cu_2O formation and its high resistance. Once the layer of Cu_2O is formed on the surface of bare copper and a series of organic film-modified electrodes, the reaction will be more difficult. Compared with the CV plots of the four electrodes, the anodic current peak II shifted gradually toward a lower potential, demonstrating that the modified electrode surfaces contain less Cu_2O, and the area of the CV curves also became gradually smaller, which indicated that the resistance of the single and complex films increased.

Table 1. Anodic peak potentials, oxidative reaction current density and the area of cyclic voltammograms.

Sample	Anodic Peak I Potential (V)	Anodic Peak II Potential (V)	Oxidative Current Density (mA/cm^2)	Area of CV Curves (10^{-4})
Blank	−0.39	−0.18/−0.13	8.416	62.8
TES	−0.33	−0.12	0.312	18.0
TES/OTES	−0.31	−0.07	0.196	4.77
TES/HDTMS	−0.29	−0.06	0.173	2.51

3.6. Potentiodynamic Polarization

Figure 7 displays the potentiodynamic polarization curves for the copper alloy electrodes unmodified and modified by single and complex films in 0.5 mol/L NaCl aqueous solution. It was clearly observed that the Ecorr corresponding to the modified copper alloy shifted significantly towards the higher potential, which indicated that the single and complex films could suppress the cathodic reactions, and inhibited the entire corrosion process in the system. The corrosion current density (Icorr) also decreased from 3.45×10^{-3} A/cm^2 for the blank copper alloy to 9.89×10^{-4} A/cm^2 for the TES single film-overed surface. As for TES/OTES and TES/HDTMS complex film-covered surfaces, the changes were even more notable, with the Icorr largely reducing to 4.56×10^{-4} A/cm^2 and 3.38×10^{-4} A/cm^2. The protection efficiency (*PE*) can be calculated with the following expression.

$$PE\,(\%) = 100 \times (1 - i/i_0) \quad (1)$$

where i_0 and i represent the corrosion current density of the blank and film-modified copper alloy, respectively. The protection efficiency is 71.3% for the TES single film-modified copper alloy surface,

while the protection efficiency of the TES/HDTMS complex film-modified surface is up to 90.2%. The results revealed that with the silanization in hydrolyzed HDTMS, the anti-corrosion performance of the complex film was better than that of the TES single film.

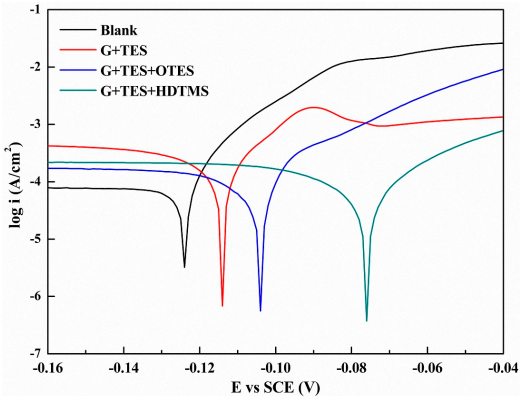


Figure 7. Potentiodynamic polarization curves for the copper alloy electrodes unmodified and modified by single and complex films in 0.5 mol/L NaCl aqueous solution.

3.7. EIS

To further evaluate the resistance property of the single and complex nanofilms, EIS was also carried out. The copper alloy electrodes with different films are immersed in 0.5 mol/L NaCl solution for 1 h before EIS measurement and bode modulus plots are depicted in Figure 8. The impedance at lower frequency is related to the corrosion inhibition property, where the higher impedance presents better corrosion protection of films for the metal substrate. Therefore, the range of 10^{-2}–10^{3} Hz was investigated especially. The impedance (|Z|) of blank, TES, TES/OTES and TES/HDTMS modified copper alloy electrodes changed from 0.73–22 Ω cm^{-2}, 1.31–1.05 × 10^{4} Ω cm^{-2}, 30.23–2.26 × 10^{4} Ω cm^{-2}, and 55.59–6.29 × 10^{4} Ω cm^{-2} in the frequency area, respectively. The plot also showed that the inductance loops appeared distinctly at 100 Hz for blank and TES film-modified copper alloy electrodes. In the meantime, the surface covered by TES/OTES complex film was also observed to show an inductance loop at 400 Hz. The appearance of the inductance loop could be attributed to the breakdown of the substrate surface which led to the serious pit corrosion. However, the behavior had not appeared on the TES/HDTMS complex film-modified electrode, indicating that the complex film protected the substrate from pit corrosion. The result is consistent with that of the potentiodynamic polarization curves.

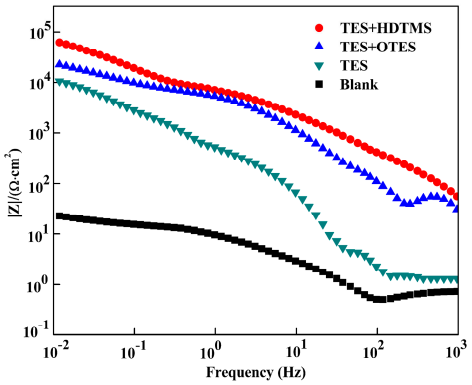


Figure 8. Bode plots for the copper alloy electrodes unmodified and modified by single and complex films in 0.5 mol/L NaCl aqueous solution.

4. Conclusions

TES single film and TES/OTES and TES/HDTMS complex films were easily constructed on a copper alloy surface based on galvanostatic electrodeposition and self-assembled methods. The hydrolyzed long-chain silane molecule could be bonded chemically with the TES electrodeposited film to increase the density of the single film, which effectively depressed the peak current for the oxidation-reduction reaction. The SEM images showed that the surface covered by TES/HDTMS complex film was more homogenous, compact, with dramatically increased film coverage, and the cyclic voltammograms, polarization curves and electrochemical impedance spectroscopy indicated that the anti-corrosion performance of the complex film was better than that of the single electrodeposited film. The TES/HDTMS complex film is expected to be applied in the metal protection fields.

Acknowledgments: The authors gratefully acknowledge the Fundamental Research Funds for the Central Universities (No. QN2013085) and the National Natural Science Foundation of China (No. 21203152).

Author Contributions: F.W. and Q.Z. conceived and designed the experiments; Q.Z. and T.T. performed the experiments; Q.Z. and F.W. wrote the paper; P.D. and Z.Z. modified the paper.

Conflicts of Interest: The authors declare no conflicts of interest.

References

1. Nunez, L.; Reguera, E.; Corvo, F.; Gonzalez, E.; Vazquez, C. Corrosion of copper in seawater and its aerosols in a tropical island. *Corros. Sci.* **2005**, *47*, 461–484. [CrossRef]
2. Gopi, D.; Govindaraju, K.M.; Prakash, V.C.A.; Sakila, D.M.A.; Kavitha, L. A study on new benzotriazole derivatives as inhibitors on copper corrosion in ground water. *Corros. Sci.* **2009**, *51*, 2259–2265. [CrossRef]
3. Meysam, S.; Abdollah, O.; Abbas, A.R.; Maryam, K. Electrodeposition and characterization of polypyrrole films on copper. *J. Electroanal. Chem.* **2010**, *645*, 149–158.
4. Zhang, Z.; Chen, S.H.; Li, Y.H.; Li, S.H.; Wang, L.H. A study of the inhibition of iron corrosion by imidazole and its derivatives self-assembled films. *Corros. Sci.* **2009**, *51*, 291–300. [CrossRef]
5. Sherif, E.M.; Park, S.M. Inhibition of copper corrosion in 3.0% NaCl solution by *N*-Phenyl-1,4-phenylenediamine. *J. Electrochem. Soc.* **2005**, *152*, B428–B433. [CrossRef]
6. Ismail, K.M. Evaluation of cysteine as environmentally friendly corrosion inhibitor for copper in neutral and acidic chloride solutions. *Electrochim. Acta* **2007**, *52*, 7811–7819. [CrossRef]
7. Li, W.H.; Zhao, X.; Liu, F.Q.; Hou, B. Investigation on inhibition behavior of *S*-triazole–triazole derivatives in acidic solution. *Corros. Sci.* **2008**, *50*, 3261–3266. [CrossRef]
8. Shukla, S.K.; Singh, A.K.; Quraishi, M.A. Triazines: Efficient corrosion inhibitors for mild steel in hydrochloric acid solution. *Int. J. Electrochem. Sci.* **2012**, *7*, 3371–3389.
9. Ashry, E.S.H.E.; Nemr, A.E.; Esawy, S.A.; Ragab, S. Corrosion inhibitors part II: Quantum chemical studies on the corrosion inhibitions of steel in acidic medium by some triazole, oxadiazole and thiadiazole derivatives. *Electrochim. Acta* **2006**, *51*, 3957–3968.
10. Montemor, M.F.; Trabelsi, W.; Zheludevich, M.; Ferreira, M.G.S. Modification of bis-silane solutions with rare-earth cations for improved corrosion protection of galvanized steel substrates. *Prog. Org. Coat.* **2006**, *57*, 67–77. [CrossRef]
11. Wang, Y.H.; Yu, Q.; Zhang, Y.; Guo, Z.; Gu, N.; Wesche, K.-D. Self-assembled monolayers of 3-mpt and its mixed-monolayers with alkanethiol on silver: Studies by xps and electrochemical methods. *Appl. Surf. Sci.* **2004**, *229*, 377–386. [CrossRef]
12. Maayta, A.K.; Fares, M.M.; Al-Shawabkeh, A.F. Influence of linear alkyl benzene sulphonate on corrosion of iron in presence of magnetic field: Kinetic and thermodynamic parameters. *Int. J. Corros.* **2010**, *2010*, 1687–9325. [CrossRef]
13. Mori, K.; Okai, Y.; Horie, H.; Yamada, H. The corrosion and inhibition of copper powders. *Corros. Sci.* **1991**, *32*, 1237–1252. [CrossRef]
14. Mori, K.; Sasaki, H.; Kobayashi, I.; Sai, S.; Hirahara, H.; Oishi, Y. Adhesion of nylon-6 to triazine trithiol-treated metals during injection molding. *J. Adhes. Sci. Technol.* **2000**, *14*, 791–803. [CrossRef]

15. Wang, F.; Mori, K.; Oishi, Y. Electrochemical polymerization of 6-(*N*-Allyl-1,1,2,2-tetrahydroperfluorodecyl) amino-1,3,5-triazine-2,4-dithiol monosodium on aluminum. *Polym. J.* **2006**, *38*, 484–489. [CrossRef]
16. Baba, H.; Kodama, T.; Mori, K.; Hirahara, H. The corrosion inhibition of copper by potentiostatic anodization in triazinedithiol solutions. *Corros. Sci.* **1997**, *41*, 555–564. [CrossRef]
17. Li, Y.N.; Wang, D.; Zhang, H.N.; Wang, F. Study on triazinethiol electropolymerized films prepared by cyclic voltammetry and galvanostatic on copper alloy surface. *Int. J. Electrochem. Sci.* **2011**, *6*, 4404–4410.
18. Kang, Z.X.; Ye, Q.; Sang, J. Fabrication of super-hydrophobic surface on copper surface by polymer plating. *J. Mater. Process. Technol.* **2009**, *209*, 4543–4547. [CrossRef]
19. Wang, F.; Li, Y.N.; Wang, Y.B.; Cao, Z. Self-assembled monolayer of designed and synthesized triazinedithiolsilane molecule as interfacial adhesion enhancer for integrated circuit. *Nanoscale. Res. Lett.* **2011**, *6*, 483–487. [CrossRef] [PubMed]
20. Hassan, H.H. Corrosion behaviour of zinc in sodium perchlorate solutions. *Appl. Sur. Sci.* **2001**, *174*, 201–209. [CrossRef]
21. Cai, M.; Park, S.M. Oxidation of zinc in alkaline solutions studied by electrochemical impedance spectroscopy. *J. Electrochem. Soc.* **1996**, *143*, 2125. [CrossRef]
22. Chen, Y.; Chen, S.; Yu, F.; Sun, W.W.; Zhu, H.Y.; Yin, Y.S. Fabrication and anti-corrosion property of superhydrophobic hybrid film on copper surface and its formation mechanism. *Surf. Interface Anal.* **2009**, *41*, 872–877. [CrossRef]



© 2016 by the authors; licensee MDPI, Basel, Switzerland. This article is an open access article distributed under the terms and conditions of the Creative Commons Attribution (CC-BY) license (http://creativecommons.org/licenses/by/4.0/).